JOURNAL OF APPLIED TOXICOLOGY
J. Appl. Toxicol. 19, S59–S70 (1999)

Development of Reactive Topical Skin Protectants against Sulfur Mustard and Nerve Agents

Olga Koper, Eric Lucas and Kenneth J. Klabunde*
Nantek, Inc., 1500 Hayes Drive, and Department of Chemistry, Kansas State University, Manhattan, KS 66502, USA

Key words: reactive nanoparticles; GA; GB; HD; VX; topical skin protectant; metals; metal oxides.

The potential for highly reactive nanoparticles (RNP) to absorb destructively, i.e. to neutralize highly toxic substances such as the warfare agents GA, GB, HD and VX, has been demonstrated in the laboratory. Reactive nanoparticles represent a new class of nanoscale particles of metals and metal oxides that differ from other nanoparticles in reactivity and crystalline morphology.

The potential for incorporating RNP into a protective barrier skin cream also has been demonstrated. Preliminary studies indicate that RNP are physically and chemically compatible with a base cream provided by the Army Medical Research Office and, importantly, remain reactive with chemical agents while promising to be compatible with skin contact.

INTRODUCTION

Introduction to Nantek's destructive adsorption technology

The need for military personnel protective systems capable of neutralizing highly toxic substances such as the warfare agents GA, GB, HD, and VX has been identified as a significant problem facing the Department of Defense.[1–24] For the specific application addressed in this paper, reactive adsorbent materials can be mixed into a base cream to provide protection for skin in the event of exposure to such highly toxic substances. Other counter-measures or protective uses for the adsorbents could include air purification, personnel ventilation systems and wide-area surface decontamination.

Significant work has been conducted at Kansas State University, resulting in the discovery of unique nanoparticle materials exhibiting extraordinary abilities to destroy highly toxic substances such as nerve agents, polychlorinated biphenyls (PCBs) and insecticides.[20–24] Much of the basic research in nanoparticle synthesis and reactive chemistry has been funded by a variety of federal grant sources, including the Department of Army. From this basic research focusing on the synthesis, characterization and reaction chemistry of a broad range of nanoparticle materials, several patents are pending on the unique nanoparticles and the underlying destructive adsorption technology (DAT).

Essentially, the research conducted had demonstrated the ability of the unique nanoparticles to both adsorb and destroy hazardous compounds. Initial work focused on the use of DAT as an alternative to high-temperature incineration for the bulk treatment of organophosphorus compounds, chlorinated hydrocarbons, PCBs, insecticides and other similar hazardous substances. On a laboratory scale, special metal oxide nanoparticles destructively adsorbed mimics of nerve gases, including paraoxon, one-armed mustard and dimethyl methyl phosphonate, as well as carbon tetrachloride, which is a fairly stable compound. Laboratory results strongly suggested that the nanoparticles indeed react with these substances at room temperature, thus opening the application to personal and building ventilation systems, protective skin products and wide-area surface decontamination.

The nanoparticles seem to provide a clear advantage over other competing decontamination technologies, such as activated carbon adsorbents and highly caustic solutions. Other decontaminants used primarily for surface decontamination, such as DS2, ozone and ethanol–NaOH–ammonia solutions,[25] are highly toxic for skin exposure and would not be compatible with the proposed base skin cream. Activated carbon, a possible solid adsorbent, has the disadvantages that:

(i) carbon does not destroy the toxic chemical but merely 'holds it' by weak adsorption forces;
(ii) inorganic pollutants such as hydrogen cyanide, cyanogen chloride and acid gases are not adsorbed well by activated carbon;
(iii) clean-up and disposal of the contaminated carbon is difficult because the hazardous material is believed to be only adsorbed but still highly toxic.

Caustic sorbents are obviously unsuitable for this application, posing a significant hazard for humans. In fact, the solutions used for such purposes are so highly caustic that they corrode metals, paint and wood.

Thus, new materials or adsorbents offering rapid kinetics yet suitable from a safety and cost standpoint need to be developed that can protect skin from exposure to highly toxic nerve agents when combined

* Correspondence to: K. J. Klabunde, Nantek, Inc., 1500 Hayes Drive, Manhattan, KS 66502, USA.

Received 1 October 1998

with a suitable barrier base cream. The unique nanoparticle adsorbents under development by Nantek offer significant potential in satisfying these difficult technical and economic challenges.

Purpose of the current work

The main objective was to demonstrate the chemical feasibility of nanoscale destructive adsorbents as the active ingredient for a topical skin protectant against mustard and nerve agents. To meet this objective, four specific tasks were undertaken. First, a broad array of nanoparticles were fabricated and tested under ambient conditions to identify the likely best alternatives for the topical skin protectant application. Second, compatibility of the nanoparticles within the base cream was studied, focusing primarily on suspension stability and chemical compatibility of the adsorbents was other components in the base cream. Third, the performance of the destructive adsorbents was confirmed with real military agents through limited laboratory tests conducted with a qualified independent laboratory. Finally, a prototype reactive topical skin protectant system was formulated and the reaction efficacy of the adsorbents was evaluated on a preliminary basis in the presence of the base cream ingredients.

EXPERIMENTAL

Synthesis of nanoparticle metal oxides

Typical procedures for the synthesis of nanoparticle oxides AP-MgO, AP-CaO, CP-MgO, CP-CaO and AP-TiO_2 have been reported earlier.[21c,25b,c] (AP = aerogel prepared, CP = conventionally prepared, CM = commercial samples; the AP are generally the smallest nanocrystals, ca. 4 nm, whereas the CP are usually ca. 7 nm and the CM samples are usually >20 nm.) The preparation of iron oxide-coated MgO nanocrystals, designated as $[Fe_2O_3]$AP-MgO, and $[Fe_2O_3]$AP-CaO, have also been reported.[24]

Reactivity tests

Paraoxon $[(C_2H_5O)_2PO(OC_6H_4NO_2)]$. In UV–Vis/paraoxon experiments, 0.1 g of the oxide (unless otherwise specified) was placed in a round-bottomed flask and purged with nitrogen. To the powder, organic solvent was added and the solution was again purged with nitrogen to remove moisture and air from the environment. Then, 4.5 μl of paraoxon was added and the solution was stirred with a magnetic stirrer. The mixture was sampled by removing 2 ml of the liquid at 2 min and then every 20 min up to 2 h. The disappearance of paraoxon was monitored by analyzing the UV–Vis spectra. A control (without oxide added to the flask) was carried out under the same conditions.

One-armed mustard, 2-CEES $[CH_3CH_2SCH_2CH_2Cl]$. The 2-CEES decomposition experiment was conducted in the following manner: 0.1 g of the metal oxide was placed in a round-bottomed flask attached to a glass IR cell that was subsequently evacuated (to a few millitorr of pressure). Then, 14 μl of 2-CEES was introduced via a septum on the flask. The cell was placed in the IR and the scans were taken after 5, 15 and 30 min and then every 30 min up to 5 h. The last measurement was taken after 20 h of exposure of metal oxide to 2-CEES. The appearance of vinyl sulfide, a decomposition product of 2-CEES, was observed. A blank test (without metal oxide present in the cell) showed that 2-CEES does not decompose by itself under these experimental conditions.

Skin cream/adsorbent prototype systems

Prototype skin topical protectant systems were prepared using AP-MgO as the active ingredient. Preliminary tests using Nantek's paraoxon and 2-CEES test procedures were conducted with the following results. For the paraoxon studies, 0.1 g of AP-MgO was incorporated into ca. 1.5 g of the base cream provided by the Army Medical Research Office. When paraoxon was added to the reaction flask (containing the cream mixed with a freshly distilled solvent), a color change was observed from white to yellow (similar to the results obtained during reaction with the adsorbents alone).

X-Ray diffraction studies

Powder X-ray diffraction (XRD) was carried out on a Scintiag-XDS-2000 spectrometer. The spectrometer was set at a voltage of 40 kV and a current of 40 mA. The scans were from 20° to 80°, with a scanning rate of 2° min^{-1}.

Infrared studies

Techniques for these studies of solid samples have been described previously.[5] The instrument used was an RS-1 Mattson FT-IR spectrophotometer with a liquid nitrogen-cooled detector.

Sulfur mustard (HD) and VX

Both the VX and HD tests followed the same experimental protocol. Namely, 0.1 g of AP-MgO or $[Fe_2O_3]$AP-CaO was weighed, placed in an Erlenmeyer flask and covered with parafilm (several flasks were prepared at the same time). Then, 100 ml of organic solvent was added to each flask. Thereupon, 4 or 20 μl of VX (or HD) was added and the start time was recorded. After 2 h analysis for VX (or HD) was carried out by gas chromatography with a flame photoionization detector (GC/PPD) especially set for sulfur detection. Samples were also extracted after 6 h and analyzed.

For the HD experiments, two methods were used: the same method as described above for VX; and a dry method where 4 μl of HD was injected directly onto dry AP-MgO or $[Fe_2O_3]$AP-CaO. After 6 h, the used AP-MgO or $[Fe_2O_3]$AP-CaO was extracted with an organic solvent, and analysis for HD was carried out by GC/FPD.

RESULTS AND DISCUSSION

Several unique nanoparticles were developed during this work that were believed to be possible candidates for the skin cream protectant system. These included oxides of magnesium, titanium, calcium, zinc, nickel and copper, and composite samples consisting of transition metal-coated nanoparticles.

Extensive testing of the destructive adsorbent performance of a broad array of nanoparticle samples was conducted. These tests were conducted using mimics of nerve agents such as paraoxon and 2-CEES (the one-armed mustard). Figure 1 provides an illustration of the chemical composition of the military agents and their corresponding mimics.

Decomposition of paraoxon on various metal oxides

In the initial trials, a broad array of readily available samples (either commercial samples or particles previously produced at Nantek's laboratory) were tested for paraoxon decomposition, as detailed in Table 1. Figure 2 shows the disappearance of paraoxon on these sample compounds over time. In these experiments, the reaction was monitored over a period of 24 h. After the best samples were chosen, more detailed studies of the initial reaction of the adsorbent/mimic were carried out. In addition to the UV–Vis spectra analysis, adsorption of the paraoxon was readily visible on most of the white powder samples due to the change in color of the powder from white to bright yellow. Note that paraoxon is a pale yellow, oily substance and its color does not duplicate the bright yellow observed. However, the anion $O_2NC_6H_4O^-$ is bright yellow, and this observation coupled with IR data strongly suggests that the anion is formed very quickly on the surface of some of the nanoscale oxide adsorbents.

Some general conclusions can be drawn from Fig. 2. Materials with higher surface area appear to adsorb much better than those with lower surface area; however, some discrepancies were observed. For example,

Table 1. Samples studied in preliminary mimic adsorption

Sample description	Designator	Surface area ($m^2 g^{-1}$)
Commercial copper oxide	CM-CuO	<1
Commercial nickel oxide	CM-NiO	4
Commercial iron oxide	CM-Fe_2O_3	8
Commercial zinc oxide	CM-ZnO	24
Conventionally prepared zinc oxide	CP-ZnO	20
Commercial titanium dioxide	CM-TiO_2	42

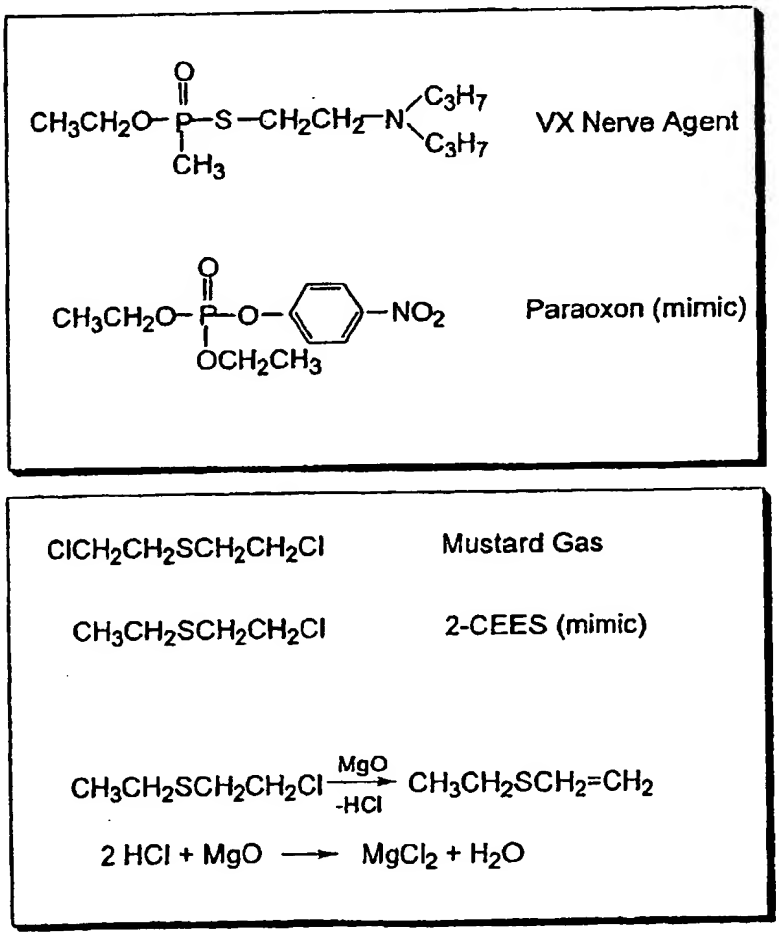

Figure 1. Military agents and their mimic counterparts.

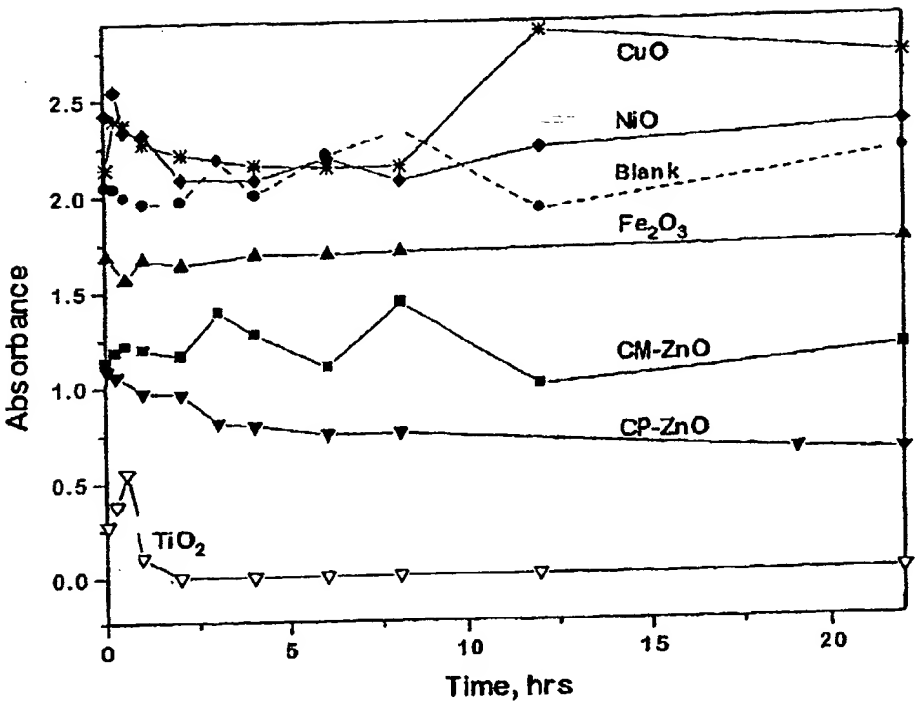

Figure 2. Rate of disappearance of paraoxon (4.5 μl) on different metal oxides (0.1 g).

the commercial zinc oxide (CM-ZnO) particles have a slightly higher surface area than Nantek's conventionally prepared (CP-ZnO) samples. However, adsorption of paraoxon is actually poorer on the higher surface area commercial samples (CM-ZnO). Particles of CM-ZnO are believed to be more spherical in microstructure, with lower reactivity compared to Nantek's conventionally prepared samples.

Titanium dioxide (TiO_2) samples were also studied and they adsorbed paraoxon reasonably well. (However, later tests with 2-CEES, the mustard mimic, were not successful, and so TiO_2 is not considered to be a good candidate for the final formulation.) Finally, moderate surface area copper and nickel oxides did not adsorb any paraoxon on the surface. Iron oxide demonstrated some adsorption capability but to a lesser extent as compared with magnesium, calcium, zinc and titanium oxide samples.

Extensive test trials. Based on the encouraging results presented above, extensive testing of the paraoxon-adsorbent reaction was conducted on a number of nanoparticle samples. The primary objective was to characterize further the performance of the adsorbents that demonstrated efficacy in the preliminary testing (i.e., CaO, MgO, ZnO and TiO_2), as well as to study the room-temperature behavior of nanoparticle composite materials. In Nantek's previous work, composite metal oxide nanoparticles coated with a monolayer of a different metal oxide (typically a transition metal) provided enhanced destructive adsorbent behavior at high reaction temperatures. The composite behavior at lower temperatures had not been characterized previously and could be of considerable interest for this protective application.

Table 2 presents the samples studied during this stage of the research. In most cases 0.1 g of metal oxide powder was used for the experiment, unless specified otherwise. The results of the paraoxon studies are found in Figs 3–6. Figure 3 shows the results of paraoxon exposure to various magnesium oxide samples, including autoclave-prepared, conventionally prepared and iron-coated composite materials. The AP-MgO nanoparticles appear to outperform all other magnesium samples tested. In particular, the paraoxon was completely adsorbed on the AP-MgO sample before the first reading could be measured at 2 min after exposure. This exceptional performance has been repeated in several test trials and is probably due to

Table 2. Samples studied for paraoxon decomposition

Sample description	Designator	Surface area $(m^2\ g)^{-1}$
Autoclave-prepared magnesium oxide	AP-MgO	562
Conventionally prepared magnesium oxide	CP-MgO	340
Iron-coated, autoclave-prepared magnesium oxide	[Fe_2O_3]AP-MgO	360
Autoclave-prepared calcium oxide	AP-CaO	112
Iron-coated, autoclave-prepared calcium oxide	[Fe_2O_3]AP-CaO	100
Conventionally prepared calcium oxide	CP-CaO	110
Iron-coated, conventionally prepared calcium oxide	[Fe_2O_3]CP-CaO	68
Zinc oxide—(I)	ZnO (I)	53
Zinc oxide—(II)	ZnO (II)	70
Zinc oxide—(III)	ZnO (III)	75
Commercial zinc oxide	CM-ZnO	24
Conventionally prepared zinc oxide	CP-ZnO	20
Titanium oxide—activated at 200°C	TiO_2 (act.)	42
Titanium oxide—not activated	TiO_2 (not act.)	44
Autoclave-prepared titanium oxide	AP-TiO_2	127

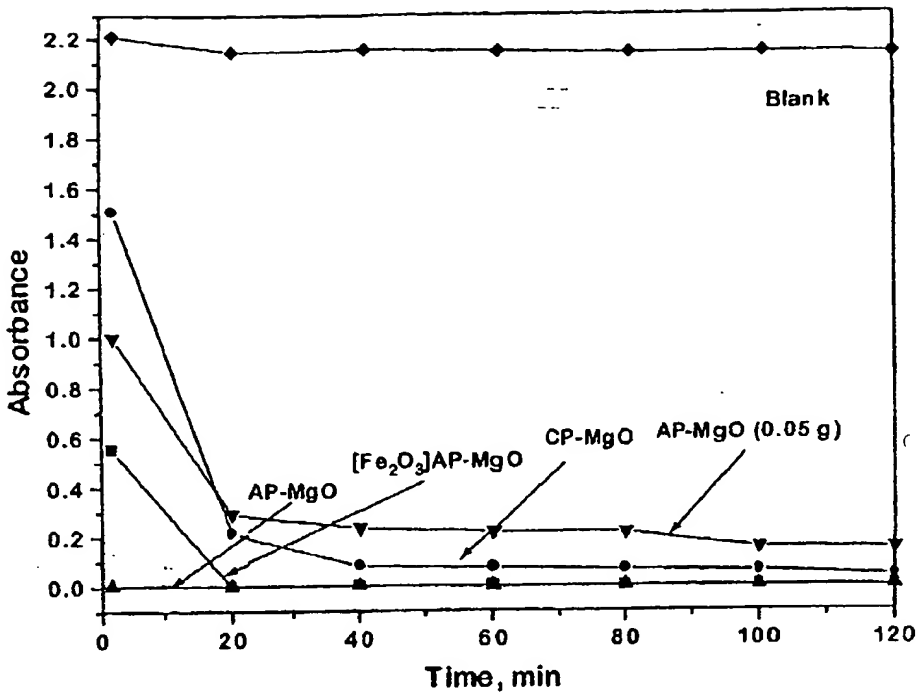

Figure 3. Rate of disappearance of paraoxon (4.5 μl) on magnesium oxide samples.

the material's very high surface area of 562 $m^2 g^{-1}$. The iron oxide-coated MgO sample ([Fe_2O_3]AP-MgO with a surface area of 360 $m^2 g^{-1}$) also behaved very well: after 20 min, no paraoxon was observed in the reaction flask. The amount of iron oxide was ca. 1% by weight of the sample. The conventionally prepared MgO samples (340 $m^2 g^{-1}$) also adsorbed paraoxon very efficiently.

The data obtained for calcium oxide are shown in Fig. 4. The iron oxide coating enhances the performance for both conventional and autoclave-prepared calcium oxide. For the iron-coated AP-CaO sample, only ca. 10% of the paraoxon was present after 2 h of reaction (based on the height of the paraoxon peak). The CP-CaO did not behave as well, even though its surface area was comparable to AP-CaO (ca. 120 $m^2 g^{-1}$). However, when iron oxide was present, the surface area of CP-CaO decreased (from 110 to 68 $m^2 g^{-1}$) but the amount of adsorbed paraoxon was much higher. The iron coating either enhances the

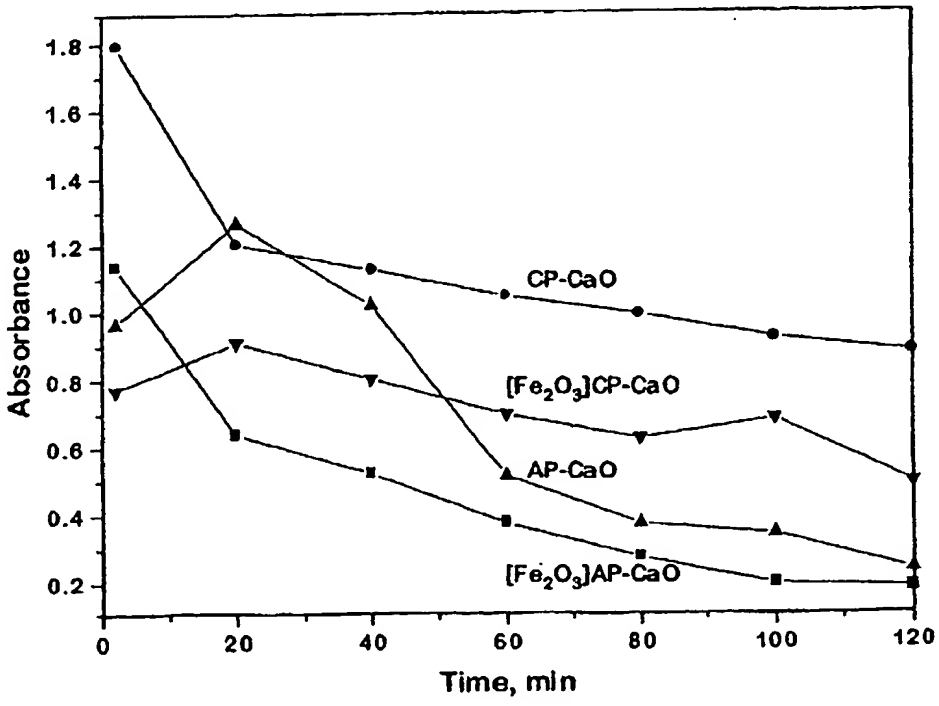

Figure 4. Rate of disappearance of paraoxon (4.5 μl) on calcium oxide samples (0.1 g).

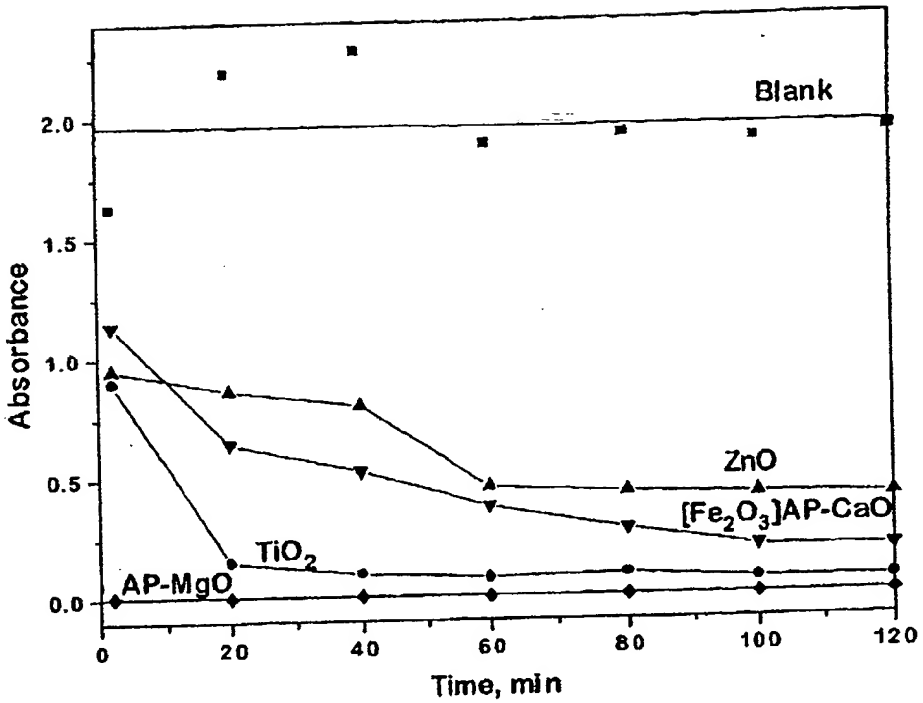

Figure 5. Rate of disappearance of paraoxon (4.5 μL) on various metal oxide samples (0.1 g).

intrinsic surface reactivity and/or it protects the core CaO particles from adventitious water, thus enhancing destructive adsorbent activity over the uncoated samples. This effect is likely to be important for the skin protection system under development, and further work is needed in order to understand this interesting effect.

Figure 5 provides data for the best oxides from each of the groups tested for the decomposition of paraoxon, as well as the blank test. In addition, Table 3 provides a tabular summary of the paraoxon decomposition 2 and 20 h after exposure. Magnesium and calcium oxides, both coated and uncoated, were very active with essentially total disappearance of paraoxon within the 20-h exposure period. In fact, for a majority of the samples, decomposition occurred very rapidly with near-complete disappearance within the first 2 h of testing. Most notably, complete disappearance of the paraoxon was observed before the initial reading at 2 min for Nantek's AP-MgO material. High-surface-area ZnO and TiO_2 also performed quite well for paraoxon decomposition.

Table 3. Decomposition of paraoxon on various metal xides after 2 and 20 h

Sample	Surface area ($m^2 g^{-1}$)	Peak intensity after 2 h	Peak intensity after 20 h
Blank	–	1.918	1.935
AP-MgO	562	0	0
CP-MgO	340	0.071	0
[Fe_2O_3]AP-MgO	360	0	0
AP-CaO	112	0.240	0
[Fe_2O_3]AP-CaO	100	0.189	0
CP-CaO	110	0.887	0.044
[Fe_2O_3]CP-CaO	68	0.487	0
ZnO (I)	53	0.406	0.229
ZnO (Ii)	70	1.729	1.628
ZnO (III)	75	0.496	
CM-ZnO	24	1.739	2.432
CP-ZnO	20	1.473	0.918
TiO_2 (act.)	42	1.412	1.297
TiO_2 (not act.)	44	1.172	1.309
AP-TiO_2	127	0	0

Sample analysis after exposure to paraoxon. After the reaction with paraoxon, a number of inspections were conducted to find additional evidence that the oxides are decomposing and not just adsorbing the toxins on the surface of the powders. As discussed earlier, adsorption of the paraoxon was readily visible on most of the white powder samples due to the change in color of the powder from white to bright yellow. This was believed to be due to the formation of the anion, $O_2NC_6H_4O^-$, which is also bright yellow. The color change was most dramatic for the magnesium samples and weakest for the low-surface-area titanium samples, correlating to the data presented above, and thus provides a clear indication that the paraoxon is being destroyed.

Solid products were studied further by XRD and IR spectroscopies. The XRD patterns did not exhibit any changes in the metal oxide structure. This was anticipated because at room temperature we would not expect much solid-state diffusion and ion–ion movement. In other words, only the surface of the oxide reacts. However, IR spectra of the solid product (IR detects the surface adsorbed species) did show some changes before and after reaction. The solid sample was studied as a pellet mixed with KBr. Some adsorptions for paraoxon disappeared upon reaction, and a strong ν_{O-H} band (3500 cm^{-1}) was present, showing the generation of new species on the surface. It is clear that the nerve agent mimic, paraoxon, has reacted

and its 'fragments' are on the surface. Further work is needed in order to elucidate what these fragments are.

Adsorption of mimics using activated carbon. We have performed preliminary benchmarking studies with a known adsorbent: activated carbon having an approximate surface area of 900 $m^2 g^{-1}$. The same test conditions were utilized during the carbon testing The activated carbon adsorbed the paraoxon well, as anticipated. After ca. 1 h, all of the paraoxon was adsorbed. However, when 10 μl of paraoxon was added to 0.1 g of the powder, only partial adsorption was observed. The same experiment was carried out with 15, 30 and 50 μl of paraoxon (per 0.1 g of activated carbon). However, in all three cases the absorbance of paraoxon was too high due to its high residual concentration, and thus out of range of the UV–Vis spectrophotometer.

For comparison purposes, similar experiments were conducted with Nantek's AP-MgO material, which has a surface area of ca. 400 $m^2 g^{-1}$. It was found that AP-MgO works much better than activated carbon, despite its lower surface area. The AP-MgO was able to adsorb/decompose completely 15 μL of paraoxon after 1 h of exposure, whereas little adsorption was observed using the activated carbon. Interestingly, when AP-MgO was used with larger amounts of paraoxon, the peak of *p*-nitrophenol, a by-product of paraoxon decomposition, became more prominent. Most likely during the decomposition, *p*-nitrophenol is formed and subsequently back-adsorbed onto the surface if enough of the surface sites are still available. When larger amounts of paraoxon were used, the formed product could not completely adsorb on the surface and was therefore released into the organic solvent. Table 4 and Fig. 6 provide additional comparative data.

After the paraoxon reaction was complete, the powders were filtered in a glove bag to minimize exposure to moisture in the atmosphere and a KBr pellet for IR studies was made. The IR spectrum of AP-MgO changes completely upon adsorption of paraoxon, and resembles the spectrum of *p*-nitrophenol adsorbed on MgO.

When the paraoxon was adsorbed on activated carbon, a very different spectrum was observed. Preliminary extraction techniques were used to characterize the surface residues on the carbon sample. Methanol, a highly polar solvent, was added to the solid product in an attempt to remove the paraoxon residue. The extract was filtered and injected into a gas chromatograph mass spectrometer for analysis. For comparison, the spectra of the starting compound, paraoxon, and the product of reaction, *p*-nitrophenol were also injected into a methanol solution. However, the methanol extraction approach was unsuccessful at removing the paraoxon species from the surface of the carbon product.

To elucidate further those species that are on the surface after reaction, other extraction procedures were attempted. Toluene was added to the solid reaction product (AP-MgO and activated carbon after reaction with 10 μl of paraoxon) and the samples were sonicated for 20 min to remove all species from the surface. The extract then was filtered using a syringe filter and injected into the gas chromatography/mass spectrometer. For AP-MgO, no additional peaks were observed; however, in the case of the activated carbon, some non-decomposed paraoxon was detected.

In summary, Nantek's AP-MgO reactant appears to adsorb significantly more than activated carbon (Aldrich, Darco G60, 100-mesh). This finding was not necessarily expected, because the carbon material with its high surface area and large pore volume is recognized for its adsorbent capability. On a preliminary basis, we attempted to confirm our belief that activated carbon adsorbs but does not react or destroy the paraoxon. We have demonstrated that special high-surface-area metal oxide materials do indeed destroy the highly toxic substances through the formation of reaction by-products, including *p*-nitrophenol for paraoxon decomposition and vinyl sulfide for the one-armed mustard decomposition. The preliminary results do indicate that the solid products are indeed quite different. New extraction techniques for elucidation of the species on the surface of the activated carbon will need to be investigated.

Table 4. Comparison of the adsorption of different amounts of paraoxon on AP-MgO. (Surface area = 400 $m^2 g^{-1}$) and activated carbon (Surface area = 900 $m^2 g^{-1}$)

Sample	Paraoxon (μl)	Intensity of the paraoxon peak after 2 h	Intensity of the paraoxon peak after 20 h
AP-MgO	4.5	0	0
AP-MgO	10	0	0
AP-MgO	15	0.027	0
AP-MgO	30	Out of range	3.543
Activated carbon	4.5	(max = 5)	0
Activated carbon	10	0	1.205
Activated carbon	15	1.520	2.729
		Out of range (max = 5)	

Decomposition of 2-chloroethylethyl sulfide (2-CEES) on various metal oxides

Extensive test trials. In these experiments the samples exhibiting the best adsorbent activity in the paraoxon studies were used to study the dehydrochlorination of 2-chloroethylethyl sulfide (2-CEES), a mimic of mustard gas. This process can be monitored using IR spectroscopy by observing the growth of a peak assigned to ethylvinyl sulfide, a decomposition product. It is necessary to observe the product of the reaction because the disappearance of 2-CEES cannot be monitored directly, owing to the majority of the peaks of 2-CEES superimposing the peaks of ethylvinyl sulfide. The only significant difference between 2-CEES spectrum and ethylvinyl sulfide spectrum is the peak at 1595 cm^{-1} attributed to the double bond of ethylvinyl sulfide. The observation of the growth of this peak was therefore used as a fingerprint in the decomposition of 2-CEES.

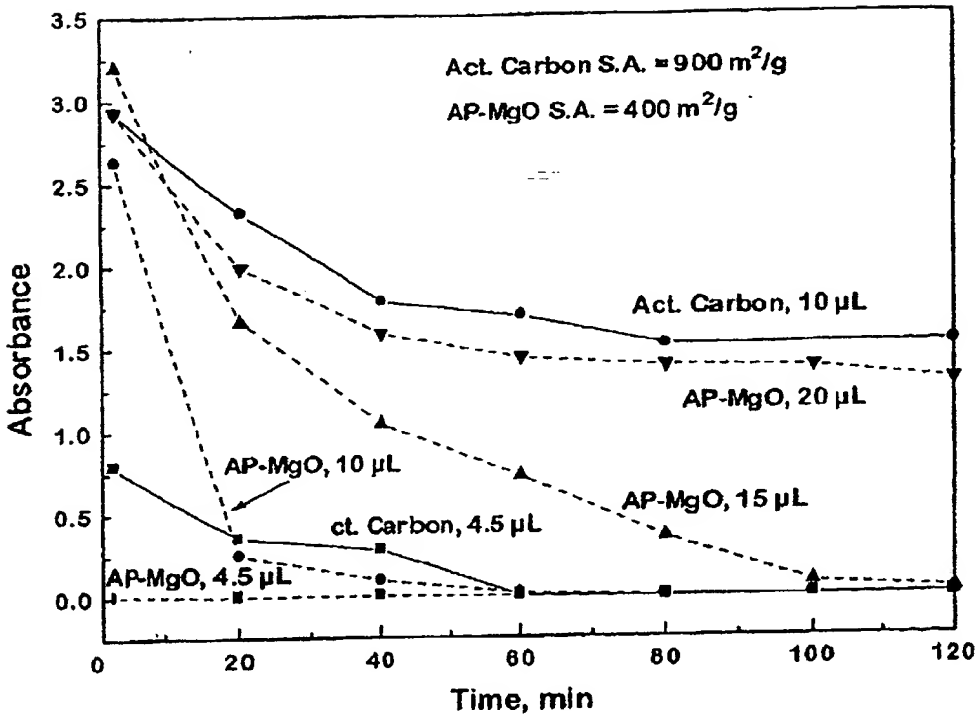

Figure 6. Adsorption/decomposition of different amounts of paraoxon on activated carbon and Nantek's AP-MgO reactants. Lower absorbance indicates more destructive adsorption of paraoxon.

The test results are presented in Table 5 and Fig. 7 for the calcium, magnesium and zinc oxide reactants. Figure 7 shows the comparison between the different types of metal oxides used and Table 5 gives the intensity of the ethylvinyl sulfide peak after 5 and 20 h of exposure. It should be noted that the 2-CEES decomposition test measures a decomposition product. Thus, increased intensity versus time suggests higher decomposition activity.

It is particularly interesting that the CaO samples are very reactive, especially the iron oxide-coated sample, [Fe_2O_3]AP-CaO. Also note that ZnO(iii) produced with a minimal amount of water is superior to ZnO(i). We are currently developing continuously improved methods of preparation of higher surface area ZnO, and believe that these results encourage further work to be done on specialized ZnO synthesis. Titanium oxide, either commercial or autoclave-prepared, did not show any activity towards 2-CEES despite the fact that it was very reactive when exposed to paraoxon. As such, further development of titanium oxide-reactive nanoparticles is not warranted.

A rather peculiar result is that the best sample for paraoxon destructive adsorption (AP-MgO) behaved unexpectedly in the 2-CEES reaction. In a very short time, ethylvinyl sulfide appeared in the spectrum, but it did not increase over time as with the other samples tested. Recall that the surface area of AP-MgO is very high (>500 $m^2\ g^{-1}$). We suspect that this curious result is due to the establishment of a rapid equilibrium where 2-CEES is destroyed, but the ethylvinyl sulfide is also largely adsorbed on the AP-MgO surface. This tentative conclusion, of course, needs further confirmation. Indeed, recent results indicate that under these experimental conditions 85% of the total 2-CEES was destroyed. Complete destruction may be inhibited by back-adsorption of the ethylvinyl sulfide. Additional efforts will be directed at this problem; new nanoparticle formulations that are more reactive with 2-CEES but less able to back-adsorb the vinyl compound will be targeted.

Similar behavior was observed for the CP-MgO sample, but to a lesser extent. In other words, back-adsorption of ethylvinyl sulfide occurred at a lower rate than that observed during the AP-MgO experiments. This is possibly attributed to the lower surface area of the CP-MgO material.

Table 5. Formation (intensity) of the ethylvinyl sulfide peak during 2-CEES decomposition on various metal xides

Sample	Surface area ($m^2\ g^{-1}$)	Absorbance after 5 h	Absorbance after 20 h
[Fe_2O_3]AP-CaO	100	58.3	186.1
CP-CaO	110	52.2	130.5
AP-CaO	92	39.1	113.3
ZnO(i)	53	14.7	34.7
ZnO(iii)	75	30.0	73.9
AP-MgO	562	20.6	52.5
CP-MgO	340	19.9	41.1
AP-TiO_2	127	0	0

Sample analysis after exposure to 2-CEES. The solid products of reaction were studied by XRD and IR spectra for evidence of decomposition. As with paraoxon decomposition, no metal oxide structural changes were observed by XRD due to the small ratio of 2-CEES to metal oxide. On the other hand, IR spectroscopy showed some differences between the

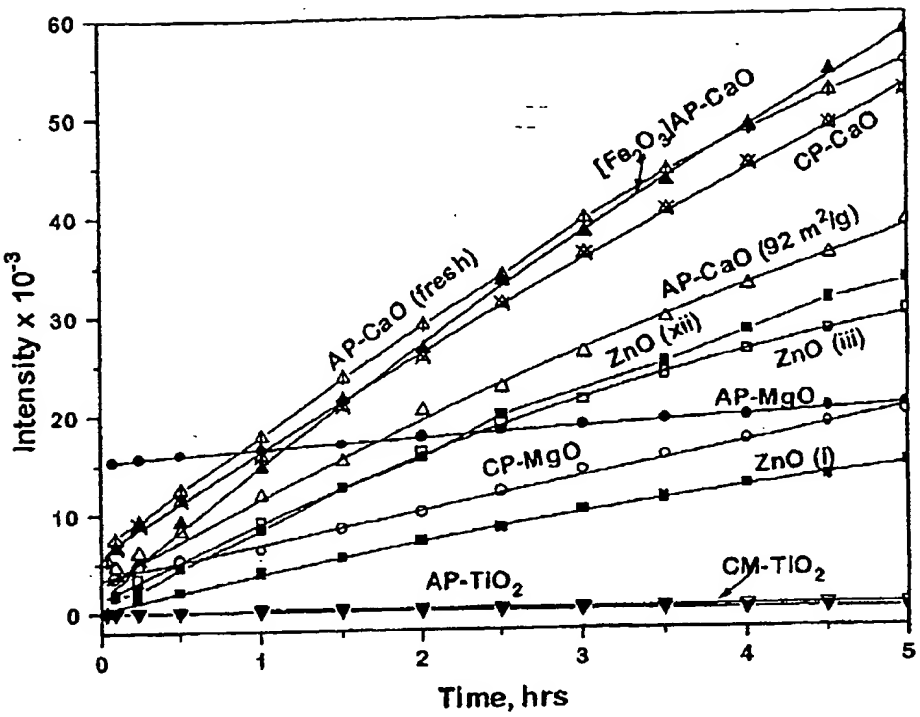

Figure 7. Appearance of ethylvinyl sulfide during 2-CEES decomposition on various metal oxides. Higher intensity indicates more destructive adsorption of 2-CEES.

oxides before and after exposure to 2-CEES. First we observed the formation of associated hydroxyl groups, as seen by the growth of a broad band at 3300 cm^{-1}; secondly, we observed the broadening of a peak at 1082 cm^{-1} (assigned to calcium carbonate on the surface of CaO). To emphasize these differences, we removed the IR spectrum of the oxide before reaction from the spectrum of the same oxide after reaction. Although the differences appear more pronounced, they did not correspond to a simple adsorption of 2-CEES or ethylvinyl sulfide on the surface. Therefore, it is clear that the mustard mimic, 2-CEES, is not simply adsorbed. It is destroyed on the surface of the nanoscale oxide particles.

Physical compatibility of the metal oxides in the base cream

Magnesium, calcium and zinc oxides were mixed with the base cream provided by the Army and XRD of the paste was taken. For comparison, a diffraction pattern of the pure cream was also recorded. The cream by itself gives a high baseline in the spectrum. However, if enough oxide is present in the cream, it is possible to distinguish between the oxide pattern and the base cream. It appears that the cream does not change upon mixing with the oxide but the spectrum of MgO coincides with the cream spectrum. On the other hand, calcium oxide and zinc oxide give clearly distinctive peaks at different angles than the cream, as is shown in Fig. 8. The stability of the oxide in the base cream was studied further using XRD spectrum analysis after exposure to the atmosphere. Specifically, the XRD spectra of calcium oxide embedded in the

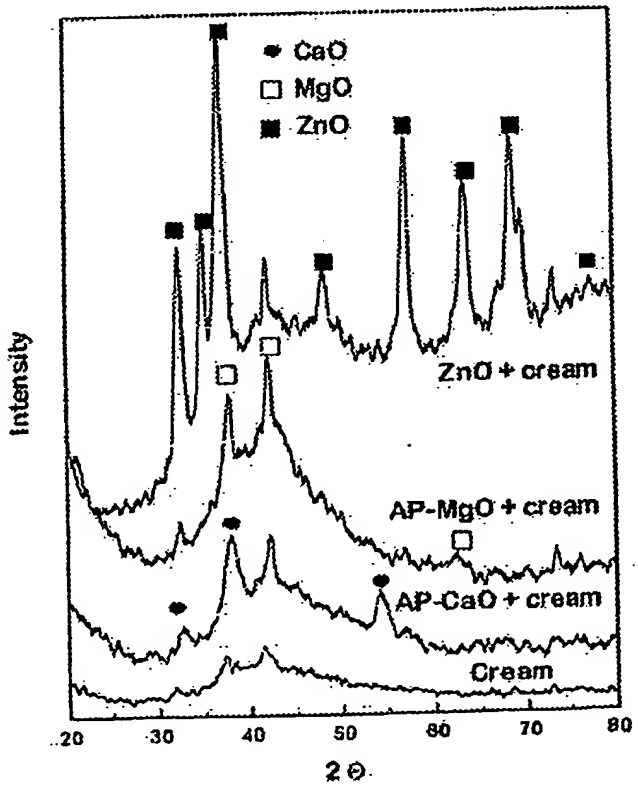

Figure 8. X-ray diffraction spectra of a skin cream system composed of metal oxides embedded in the base cream.

base cream were taken over varying times of exposure to air, with no significant changes observed.

As expected, the rate of the reaction was slower when reactants were embedded in the base cream. Nevertheless, a decrease in the paraoxon peak intensity was observed. The chemical analysis techniques utilized had sufficient noise in the response that work will be needed to quantify better the mimic reaction with the cream/adsorbent systems. Also, additional experiments need to be developed to eliminate the solvent from the reaction. In current experiments, the reaction is studied using a UV–Vis spectrophotometer with paraoxon dissolved in the solvent as the starting material and *p*-nitrophenol as the product of reaction. Such gas-phase measurements of paraoxon alone using this method are not possible due to its low vapor pressure. The solvent, however, did not appear to dissolve any of the base cream.

Preliminary test results for the destructive adsorption of the mustard mimic, 2-CEES, were also very encouraging. As with paraoxon, the adsorbent/cream mixture reacted with the mimic albeit at a slower rate than observed during the earlier adsorbent studies. It is believed that the cream is forming a barrier for the nerve agents, thus slowing the availability of the mimic to the adsorbent surface sites. Refer to Fig. 9 for a comparison of the formation of the decomposition product, ethylvinyl sulfide, for calcium and magnesium oxide adsorbents with and without the addition of the base cream.

Testing with real agents in collaboration with a qualified independent laboratory

Nantek's AP-MgO destructively adsorbed VX completely for both 4 μl and 20 μl loadings. Using organic solvent as an extraction medium, no VX was extracted from the used AP-MgO sample. Nantek's [Fe_2O_3]AP-CaO reactant also completely adsorbed 4 μl of VX; however, when 20 μl was used, about 60% of the VX remained after 6 h.

These experiments indicated that some of the HD has been adsorbed/destroyed, but not all of it. The AP-MgO behaved best, with ca. 50% decomposition within 6 h. However, the HD experiments were inconclusive owing to the wide variability and significant analytical noise.

These studies, however, demonstrate two important things: better formulations of nanoparticle metal oxides are needed for HD decomposition, although AP-MgO behaved exceptionally well for VX destructive adsorption; and, based on comparative studies, the mimics that we have chosen, namely paraoxon and 2-CEES, proved to be good mimics for modeling the destructive adsorption reaction with VX and HD military agents. In fact, paraoxon and VX destructive adsorption tracked very well with each other for the 4 μl and 20 μl tests. In addition, recent work on 2-CEES has shown that results are similar to HD, i.e. partial (85%) destruction over 6 h was observed.

It should be emphasized that for these initial tests comparatively large amounts of mimics or military nerve agents were used. These are very demanding tests, and the fact that some HD was not destroyed should not be discouraging. Further research on new, more reactive nanoparticle formulations, as well as using more realistic ratios of mimics or agents to adsorbent, needs to be carried out.

Conclusions and major findings of the research

A broad series of nanoscale metal oxides, as well as activated carbon, have been studied for destructive

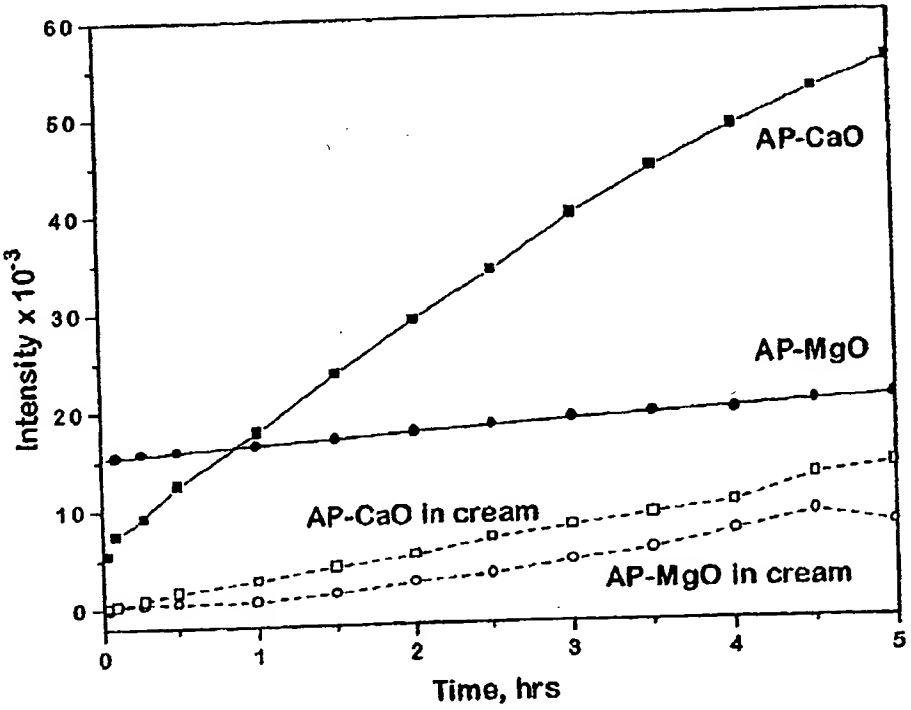

Figure 9. Appearance of ethylvinyl sulfide during the mustard mimic, 2-CEES, reaction on metal oxides with and without the base cream.

adsorbance during this effort. The following represents the major findings.

Identification of suitable nanoscale reactive adsorbent materials

The best formulations appear to be AP-MgO, [Fe_2O_3] AP-CaO and CP-CaO. At this time AP-MgO alone or in combination with a different metal oxide coating appears to be the most suitable reactive adsorbent for the topical skin cream application. However, substantial work is still needed to understand the products of the reaction, to custom design the most reactive adsorbent and to improve incrementally the reaction kinetics, especially to improve performance with HD.

Based on the preliminary paraoxon and 2-CEES decomposition studies, iron oxide coated CaO, coated and uncoated AP-MgO and high-surface-area ZnO provide significant promise for a reactive adsorbent in the skin protectant application. The Fe_2O_3 coating provides enhanced reaction, possibly due to a catalytic effect and/or due to the prevention of hydroxylation of the oxide powders.

As discussed previously, the enhancing effect of the outer metal oxide coating (the shell material of these core/shell nanoparticles) could be due to a catalytic effect where the outer oxide shuttles fragments of the mimic into the core oxide, where it is consumed. This catalytic effect has been demonstrated clearly in high-temperature (400–500°C) destructive adsorption work, but now appears to be viable possibly at room temperature as well. Further work to delineate the true function of the shell oxide (catalytic shuttle or protectant against hydrolysis or some other subtle effect) will be carried out in the future.

Autoclave-prepared MgO samples showed remarkable performance. These particles are the highest surface area samples tested, with a surface area of $>500\ m^2\ g^{-1}$. For the paraoxon studies, the AP-MgO nearly instantaneously destructively adsorbed all of the paraoxon before the first reading at 2 min after exposure. For the 2-CEES studies, it appears that the oxide reached a rapid equilibrium in <5 min where much of the 2-CEES was destroyed, but the ethylvinyl sulfide was also absorbed on the particle surface. This result shows the need to develop additional tests suited for the case where rapid adsorption of both the starting material and products of reaction occurs. In addition, the solid samples of reacted AP-MgO were studied and significant evidence of reaction or destructive adsorption of the paraoxon was observed.

Comparison of nanoscale reactive particles with activated carbon

Although evidence of actual destruction of the mimic compound was observed for many of Nantek's custom reactive adsorbents, we were able to confirm that destructive adsorption does not take place using activated carbon, a well-known highly adsorbent material. Activated carbon seems to adsorb quickly both paraoxon and 2-CEES; however, no evidence of decomposition of the mimic compounds was observed. An unexpected outcome of the research was that activated carbon actually has a lower adsorption capacity than Nantek's AP-MgO material on an equivalent gram basis. When 0.1 g of each adsorbent was used, only 4.5 μl of paraoxon was completely adsorbed on the activated carbon surface whereas the AP-MgO adsorbed/destroyed 20 μl of paraoxon.

Decomposition of the military nerve agents VX and HD

Nantek's AP-MgO showed exceptional results for the destruction of VX, with complete decomposition for both 4 μl and 20 μl loadings. In addition, no VX was extracted from the used AP-MgO sample using CH_2Cl_2 as an extraction solvent. Nantek's [Fe_2O_3]AP-CaO reactant also completely adsorbed 4 μl of VX; however, when 20 μl was used, ca. 60% of the VX remained after 6 h. The HD experiments indicated that some of the HD is adsorbed upon contact with the nanoscale reactants, but not all of it. Autoclave-prepared MgO behaved the best, destroying ca. 50% of the agent.

Chemical compatibility of the adsorbents with the base cream

Several nanoscale metal oxide samples, including magnesium, calcium and zinc, demonstrated compatibility upon mixing with the base cream provided by the Army. Furthermore, no significant changes in the cream were observed using XRD analysis upon prolonged exposure to atmospheric conditions.

Decomposition of mimics upon exposure to the prototype skin cream systems

In the preliminary tests, AP-MgO appears to remain reactive upon mixing with the base cream for both paraoxon and 2-CEES exposure. Owing to the barrier nature of the base cream, the reaction occurred at a slower rate than observed when the reactants were exposed directly to the mimic compounds.

Acknowledgements

We thank Donna R. Nichols of the Midwest Research Institute for carrying out experiments with VX and HD, and the Department of the Army, US Army Medical Research and Material Command for financial support.

REFERENCES

1. (a) Y. X. Li and K. J. Klabunde, *Langmuir* **7**, 1388 (1991); (b) Y. X. Li, J. R. Schlup, K. J. Klabunde *Langmuir* **7**, 1394 (1991).
2. J. G. Ekerdt, K. J. Klabund , J. R. Shapley, J. M. White and J. T. Yates, Jr. *J. Phys. Chem.* **92**, 6182 (1988).
3. R. W. Baier and S. W. Weller, *Ind. Eng. Chem. Process Des. Dev.* **6**, 380 (1967).
4. W. M. Graven, S. W. Weller and D. L. Peters, *Ind. Eng. Chem. Process Des. Dev.* **5**, 183 (1966).
5. R. L. Parfitt and J. D. Russell, *J. Soil Sci.* **28**, 297 (1977).
6. L. Lyklema, *Environ. Sci. Technol.* **14**, 297 (1980).
7. W. Strumm, G. Furrer and B. Kunz, *Croat. Chem. Acta* 585 (1983).
8. W. M. Graven, J. D. Paton and S. W. Weller, *Ind. Eng. Chem. Process Des. Dev.* **5**, 34 (1966).
9. V. S. Smentkowski, P. L. Hagans and J. T. Yates, Jr., *J. Phys. Chem.* **92**, 6352 (1988).
10. V. S. Smentkowski, P. L. Hagans and J. T. Yates, Jr., *US Patent No. 4,871,526.*
11. X. Guo, J. Yoshinobu, and J. T. Yates, Jr., *J. Phys. Chem.* **94**, 6839 (1990).
12. C. S. Dulcey, M. C. Lin and C. C. Hsu, *Chem. Phys. Lett.* **115**, 481 (1985).
13. R. I. Hegde, C. M. Greenlief and J. M. White, *J. Phys. Chem.* **89**, 2886 (1986).
14. M. A. Henderson and J. M. White, *J. Phys. Chem.* **110**, 6939 (1988).
15. R. I. Hegde and J. M. White, *Appl. Surf. Sci.* **28**, 1 (1987).
16. M. A. Henderson, T. Jin and J. M. White, *J. Phys. Chem.* **90**, 4607 (1986).
17. M. K. Templeton and W. H. Weinberg, *J. Am. Chem. Soc.* *107*, 97 (1985).
18. M. K. Templeton and W. H. Weinberg, *J. Am. Chem Soc.* **107**, 774 (1985).
19. A. E. T. Kuiper, J. J. G. M. van Bokhoven and J. Medema, *J. Catal.* **43**, 154 (1976).
20. Y. X. Li, O. Koper, M. Atteya and K. J. Klabunde, *Chem of Mater.*, *4*, 323 (1992).
21. (a) S. T. Lin and K. J. Klabunde, *Langmuir* **1**, 600 (1985); (b) K. J. Klabunde and H. Matsuhashi, *J. Am. Chem. Soc.* **109**, 1111 (1987); (c) K. J. Klabunde, M. F. Hoq, F. Mousa and H. Matsuhashi, *Preparative Chemistry Using Supported Reagents*, Ed. by P. Laszlo, p. 35. Academic Press, New York (1987); (d) I. Nieves and K. J. Klabunde, *Mater. Chem. Phys.* **18**, 485; (1988); (e) S. Utampanya, K. H. Klabunde and J. R. Schlup, *Chem. Mater.* **3**, 175 (1991); (f) M. Atteya and K. J. Klabunde, *Chem. Mater.* **3**, 182 (1991).
22. T. Collins, A. Held and R. Rainbolt, *Metal Oxide Particles: Detoxification of Nerve Gases*, Chemical Engineering System Design 2, ed. by W. Walawender (1993).
23. K. J. Klabunde, A. Khaleel and D Park, *High Temp. Mater. Sci*, **33**, 99–106 (1995).
24. K. J. Klabunde, J. Stark, O. Koper, C. Mohs, D. G. Park, S. Decker, Yi Jiang, I. Lagadic and D. Zhang, *J. Phys. Chem*, **100**, 12142–12153 (1996).
25. (a) Y. C. Yang, J. A. Baker and J. R. Ward, *Chem. Rev.*, **92**, 1729–1743 (1992); (b) O. B. Koper, I. Lagadic, A. Volodin and K. J. Klabunde, *Chem. Mater.*, **9**, 2468 (1997); (c) K. J. Klabunde and C Mohs, *Chemistry of Advanced Materials: an Overview*, Ed. by L. V. Interrante and M. J. Hampden-Smith, pp. 271–327. Wiley-VCH, Berlin (1998).
26. N. S. Gajbhiye, U. Bhattacharya and V. S. Darshane, *Thermochim Acta* **264**, 219–230 (1995).
27. S. C. Goel, M. Y. Chiang, P. C. Gibbons, W. E. Buhro, *Mater. Res. Soc. Symp. Proc.* **271**, 3–13 (1992).
28. M. Ohyama, H. Kozuka, K. Yoko and S Sakka, *J. Ceram. Soc. Jn.* **104**, 296–300 (1996).
29. L. Spanhel and M. A. Anderson, *J. Am. Chem. Soc., 113*, 2826–2833 (1991).
30. S. Sakohara, L. D. Tickanen and M. A. Anderson, *J. Phys. Chem.*, **96**, 11086–11091 (1992).
31. R. Lauf and W. D. Bond, *Ceram. Bull. 63*, 278–281 (1984).
32. R. H. Heistand and Y. H. Chia, *Mater Res. Soc. Symp. Proc., 73*, 93–98 (1993).
33. J. M. Burlitch, S. E. Hayes and G. E. Whitwell, *Organometallics*, **1**, 1074–1083 (1982).
34. S. Fujita, M. Usui, H. Ito and N. Takezawa, *J. Catal.*, **157**, (1995) 403–413.
35. L. Ruixia, W. Peiying and W. Shiliang, *Varistor Tech.* 117–120.
36. L. Spanhel, *Eurogel '91 Proc.*, pp. 407–414 (1992).
37. C. D. E. Lakeman and D. A. Payne, *Mater. Chem. Phys.*, **38**, 305–324 (1994).
38. B. Unger, P. Popp, U. Schade and M. Hahnert, *J. Non-Cryst.Solids*, **160**, 152–161 (1993).
39. S. Decker and K. J. Klabunde *J. Am. Chem. Soc.*, **118**, 12465–12466 (1996).